NUMERICAL IMPLEMENTATION OF HEAT EQUATION CONSIDERING NONLINEAR HEAT SOURCE

Nasser S. Alkmim

Lineu J. Pedroso

nasser.alkmim@gmail.com

lineu@unb.com.br

Universidade de Brasília, Departamento de Engenharia Civil e Ambiental - Grupo de Dinâmica e Fluido-Estrutura (GDFE). Caixa Postal 04493, Campus Darcy Ribeiro, CEP 70919-970, Brasilia-DF

Asa Norte, Brasília, 70910-900, DF, Brazil

Abstract. *In this work a numerical model for the thermal problem with nonlinear heat source is presented. The model is solved in two dimensions using finite element method and its solution is implemented using the python programming language. The nonlinear aspect of the model takes into account the heat released in a chemical reaction which is thermally activated, which means that it is affected by the temperature. The model can be useful on modeling concrete thermal behavior at early ages which is an important phenomena in large concrete structure due its impact on the integrity of the material.*

Keywords: *Concrete, Hydration, Numerical methods, Finite element method, Python*

1 INTRODUCTION

The hardening process of fresh concrete occurs due an exothermic chemical reaction, cement hydration. The heat produced by the chemical process results in a temperature increase under adiabatic conditions up to 50 $^{\circ}\mathrm{C}$, (Cervera et al., 1999). Thermal stresses arise due restrained volumetric changes. In the early ages, the volumetric expansion generates moderate compressive stresses because the stiffness of the material still in development. As the structure starts to cool down, the stiffness is well developed and the thermal gradients resulted from the interaction of the structure with its surroundings may generate considerable tensile stress. The structure is then subject to suffer damage from thermal stresses. Hence, the modeling and prediction of thermal effects on the structure are important to the monitoring aspect of engineering practice.

The hydration reaction is affected by many factors such as the cement particle size, cement quantity, water cement ratio, presence of additives, hardening state and temperature, (Reinhardt et al., 1982). The effect of the later is explored in this work. The temperature affects the chemical reaction in a non-linear way. The reaction is said to be thermal-activated, meaning that higher temperatures causes that reaction rate to increase.

Many approaches have been proposed in the literature. The coupling model between thermal, chemical and mechanical effects were described in Ulm and Coussy (1995), Cervera et al. (2002), De Schutter (2002), and Faria et al. (2006). The hydration model presented in Cervera et al. (2002) is implemented is this work. It is based on the combination of the Arrhenius equation and a mathematical function that takes into account the affinity of the chemical reaction and the permeability of water through the hydrates.

This work is mainly interested in modeling and numerically solve the thermal problem considering the non linear thermal heat released in the chemical reaction. The numerical solution is obtained via space discretization using the Finite Element Method and time discretization with Finite Differences. There are a two scale nonlinearity, one at the element level regards the reaction degree and the other, at the structure level, the temperature. The reaction degree is obtained iteratively via the Newton-Raphson method and the temperature is computed using Picard's iterative scheme due its simplicity.

2 MATHEMATICAL MODELING

The mathematical model that describes the heat transfer problem is presented in the following equation, the notation used is based on Tonti (2013), Zienkiewicz and Taylor (2000), and Rao (2011),

$$\rho c_p \partial_t T + \nabla \cdot \boldsymbol{q} \overset{\text{law}}{=} \sigma_q(T) \tag{1}$$

where, $T(\boldsymbol{x}, t)$ is the temperature field in $^{\circ}\mathrm{C}$, $\boldsymbol{q}$, in $\mathrm{W/m^2}$, is the heat current density, ρ and c_p are the material density in $\mathrm{kg/m^3}$and specific heat in $\mathrm{J/kg \cdot ^{\circ}C}$and $\sigma_q(T)$ is a temperature dependent heat source density in $\mathrm{W/m^3}$. The first term in Eq. (1) represents the change in time of the internal energy density, the second term accounts for the net heat current density, or net heat flux, in a point, the third term represents the internal heat source. So, the equation can be read as the change internal thermal energy plus the net heat flux going in the body is equal the internal heat generation. The heat current density is given by the material law

$$\boldsymbol{q} \overset{\text{mat}}{=} -\lambda \nabla T \tag{2}$$

where λ is the thermal conductivity given in $\mathrm{W/m \cdot ^\circ C}$. The notation used is recommended by Cohen et al. (1987).

The conductivity and specific heat are assumed to be constant even though they can be assigned as a function in the program.

The boundary condition can be of three major types: temperature specified in the boundary S_1, heat current density specified at S_2 and convection heat interface at S_3. The boundary conditions are,

$$T(\boldsymbol{x}, t) = T_h(t), \qquad \boldsymbol{x} \in S_1 \tag{3}$$

$$-\lambda \nabla T \cdot \boldsymbol{n} = q_h(t), \qquad \boldsymbol{x} \in S_2 \tag{4}$$

$$-\lambda \nabla T \cdot \boldsymbol{n} = h\left(T(t) - T_a(t)\right), \qquad \boldsymbol{x} \in S_3 \tag{5}$$

where h is the surface conductance, in $\mathrm{W/m^2 \cdot ^\circ C}$, T_a is the air temperature, q_h is the surface heat current specified. The initial condition is $T(\boldsymbol{x}, 0) = T_0$. A positive boundary flux means that the temperature gradient is opposite of the normal vector at the boundary, which turns out to be true when the outside temperature is lower than inside temperature. The temperature difference indicates that the heat current is going outside the domain, thermal energy is leaving the body. Note that those parameters usually change in time and the current implementation supports conditions passed as function of time.

2.1 Weak form

The weak form can be obtained using the Galerkin method, as described in Rao (2011, p. 482) and in Nithiarasu et al. (2016, p. 93).

$$\int_{\overset{e}{V}} N_i \left(\lambda \nabla \cdot \nabla T + \sigma_q - \rho c_p \partial_t T\right) \mathrm{d}V = 0, \qquad i = 1, 2, 3, 4. \tag{6}$$

Using the product rule of derivative the first term of the integral becomes

$$\int_{\overset{e}{V}} N_i \frac{\partial}{\partial x}\left(\lambda \frac{\partial T}{\partial x}\right) \mathrm{d}V = -\int_{\overset{e}{V}} \frac{\partial N_i}{\partial x} \lambda \frac{\partial T}{\partial x} \mathrm{d}V + \int_{\overset{e}{S}} N_i \lambda \frac{\partial T}{\partial x} l_x \, \mathrm{d}S \tag{7}$$

where l_x is the direction cosine of the outward normal to the domain surface. Substituting that into Eq. (6),

$$-\int_{\overset{e}{V}} \lambda \nabla N_i \cdot \nabla T \, \mathrm{d}V + \int_{\overset{e}{S}} N_i \lambda \nabla T \cdot \boldsymbol{n} \, \mathrm{d}S + \int_{\overset{e}{V}} N_i \left(\sigma_q - \rho c_p \partial_t T\right) \mathrm{d}V = 0 \qquad i = 1, 2, 3, 4. \tag{8}$$

Using the weak form of the two Neumann boundary conditions, the surface integral becomes

$$\int_{\overset{e}{S}} N_i \lambda \nabla T \cdot \boldsymbol{n} \, \mathrm{d}S = -\int_{\overset{e}{S_2}} N_i q_h \, \mathrm{d}S - \int_{\overset{e}{S_3}} N_i h (T - T_a) \, \mathrm{d}S \tag{9}$$

substituting this value in Eq. (8)

$$-\int_{\overset{e}{V}} \lambda \nabla N_i \cdot \nabla T \, \mathrm{d}V - \int_{\overset{e}{S_2}} N_i q_h \, \mathrm{d}S - \int_{\overset{e}{S_3}} N_i h (T - T_a) \, \mathrm{d}S + \int_{\overset{e}{V}} N_i \left(\sigma_q - \rho c_p \partial_t T\right) \mathrm{d}V = 0 \qquad i = 1, 2, 3, 4. \tag{10}$$

Dropping the element superscript (e), and rearranging the terms in the above equation,

$$\int_V \lambda \nabla N_i \cdot \nabla T \, \mathrm{d}V + \int_V \rho c_p \partial_t T \, \mathrm{d}V + \int_{S_2} N_i q_h \, \mathrm{d}S + \int_{S_3} N_i h (T - T_a) \, \mathrm{d}S - \int_V N_i \sigma_q \, \mathrm{d}V = 0 \qquad i = 1, 2, 3, 4. \quad (11)$$

Breaking the convection term apart,

$$\int_V \lambda \nabla N_i \cdot \nabla T \, \mathrm{d}V + \int_V \rho c_p \partial_t T \, \mathrm{d}V + \int_{S_2} N_i q_h \, \mathrm{d}S + \int_{S_3} N_i h T \, \mathrm{d}S - \int_{S_3} N_i h T_a \, \mathrm{d}S - \int_V N_i \sigma_q \, \mathrm{d}V = 0 \qquad i = 1, 2, 3, 4. \quad (12)$$

Rearranging the terms,

$$\int_V \lambda \nabla N_i \cdot \nabla T \, \mathrm{d}V + \int_V \rho c_p \partial_t T \, \mathrm{d}V + \int_{S_3} N_i h T \, \mathrm{d}S = \int_V N_i \sigma_q \, \mathrm{d}V - \int_{S_2} N_i q_h \, \mathrm{d}S + \int_{S_3} N_i h T_a \, \mathrm{d}S \qquad i = 1, 2, 3, 4. \quad (13)$$

2.2 Finite element equations

The finite element equations for the transient heat problem, as described in Rao (2011, p. 481), with different notation,

$$\boldsymbol{K}_s^e \dot{\boldsymbol{T}}^e + \left[\boldsymbol{K}_q^e + \boldsymbol{K}_c^e\right] \boldsymbol{T}^e = \boldsymbol{p}^e(T) \quad (14)$$

where $\boldsymbol{T}^e$ is the unknown vector containing the nodal values for the temperature field, $T(\boldsymbol{x}, t)$, K_s^e is the element matrix due internal thermal energy storage, also known as capacitance matrix, $\boldsymbol{K}_q^e$ is the element matrix due heat current density (heat flux), also known as condutance matrix because the main contribution comes from thermal conductivity, and $\boldsymbol{K}_c^e$ is the element matrix due the convection term. The element matrices are given by

$$\boldsymbol{K}_s^e = \int_{\overset{e}{V}} \bar{\boldsymbol{N}}^T \rho c_p \bar{\boldsymbol{N}} \, \mathrm{d}V \quad (15)$$

$$\boldsymbol{K}_q^e = \int_{\overset{e}{V}} \bar{\boldsymbol{B}}^T \lambda \bar{\boldsymbol{B}} \, \mathrm{d}V \quad (16)$$

$$\boldsymbol{K}_c^e = \int_{\overset{e}{S_3}} h \bar{\boldsymbol{N}}^T \bar{\boldsymbol{N}} \, \mathrm{d}S \quad (17)$$

$$\boldsymbol{p}^e(T) = \int_{\overset{e}{V}} \bar{\boldsymbol{N}}^T \sigma_q(T) \, \mathrm{d}V - \int_{\overset{e}{S_2}} \bar{\boldsymbol{N}}^T q_h \, \mathrm{d}S + \int_{\overset{e}{S_3}} \bar{\boldsymbol{N}}^T h T_a \, \mathrm{d}S \quad (18)$$

where, $\sigma_q(T)$ is a source of non-linearity and represents the internal heat source in $\mathrm{W/m^3}$. The term q_h is the heat current density specified at the boundary. The equivalent thermal load can be written as,

$$\boldsymbol{p}^e(T) = \boldsymbol{p}_q^e(T) - \boldsymbol{p}_t^e + \boldsymbol{p}_c^e, \quad (19)$$

where, $\boldsymbol{p}_q^e(T)$ is the equivalent load due the internal heat source, $\boldsymbol{p}_t^e$ is the equivalent load due heat current flux specified in the boundary S_2, traction equivalent of the mechanical problem, and $\boldsymbol{p}_c^e$ is the equivalent load due convective heat in boundary S_3.

Using a backward finite difference scheme, as suggested by Bofang (2014, p. 177),

$$T_{n+1} - T_n = \Delta t_n \left(\frac{\partial T}{\partial t} \right)_{n+1} \tag{20}$$

where $T_n = T(t_n)$ and Δt is the finite step size. Using the vector form of Eq. (20) and substituting the differential operator in Eq. (14) in its global form (after the assemble procedure) yields,

$$\boldsymbol{K}_s \frac{1}{\Delta t} \left[\boldsymbol{T}_{n+1} - \boldsymbol{T}_n \right] + \left[\boldsymbol{K}_q + \boldsymbol{K}_c \right] \boldsymbol{T}_{n+1} = \boldsymbol{p}(\boldsymbol{T}_{n+1}) \tag{21}$$

rewriting Eq. (21) as,

$$\hat{\boldsymbol{K}} \boldsymbol{T}_{n+1} = \hat{\boldsymbol{F}}(\boldsymbol{T}_{n+1}) \tag{22}$$

where,

$$\hat{\boldsymbol{K}} = \frac{1}{\Delta t} \boldsymbol{K}_s + \boldsymbol{K}_q + \boldsymbol{K}_c, \qquad \hat{\boldsymbol{F}}(\boldsymbol{T}_{n+1}) = \boldsymbol{p}(\boldsymbol{T}_{n+1}) + \frac{1}{\Delta t} \boldsymbol{K}_s \boldsymbol{T}_n \tag{23}$$

Because we need the temperature at t_{n+1} to compute $\boldsymbol{p}_{n+1}$, which is the non-linearity in the problem, the Newton-Raphson scheme is used.

The element temperature field interpolation functions, $\bar{\boldsymbol{N}}$, and the temperature gradient interpolation matrix, $\bar{\boldsymbol{B}}$:

$$\bar{\boldsymbol{N}} = \begin{bmatrix} N_1 & N_2 & N_3 & \dots \end{bmatrix} \qquad \bar{\boldsymbol{B}} = \begin{bmatrix} \partial_x N_1 & \partial_x N_2 & \dots \\ \partial_y N_1 & \partial_y N_2 & \dots \end{bmatrix} \tag{24}$$

2.3 Internal heat source

The internal heat source is the result of a chemical reaction of cement with water. The energy liberated in the reaction is dependent on the temperature, this reaction is then said to be thermally activated (Cervera et al., 2002; Azenha, 2009, p. 43). The hydration reaction results in hardening concrete and its status can be described by the degree of hydration $\alpha_h(t)$. The degree of hydration is the ratio between the amount of cement reacted and the total amount of cement in the mixture. Since the amount of cement is proportional to the amount of energy released, hydration heat, the degree of hydration can be expressed in terms of the heat released, (De Schutter and Taerwe, 1995; Caggiano et al., 2012). Defining the degree of reaction as

$$\alpha = \frac{Q(t)}{Q_{max}} \tag{25}$$

where $Q(t)$ and Q_{max} represent the heat of hydration released and the maximum heat of hydration release, respectively.

Reinhardt et al. (1982) indicated that the hydration heat current, $\sigma_q = \dot{Q}$, when divided by the maximum rate $\sigma_{q,max}$ is independent on the temperature. This ratio is only dependent on the degree of reaction,

$$\frac{\sigma_q}{\sigma_{q,max}} = f(\alpha) \tag{26}$$

In fact, this hypothesis is not always correct, as suggested by De Schutter and Taerwe (1995). It can be assumed so for temperatures in the range of 20 to 60 $^{\circ}$C. Azenha (p. 60 2009) points that large structures where multiple cements are blended should be treated with care when modeling the hydration reaction. The effect of the temperature on the hydration heat rate is such that higher temperatures yields an increase in the reaction rate. De Schutter and Taerwe (1995) propose the following consideration of the maximum hydration heat rate,

$$\sigma_{q,max} = \sigma_{q,max,20} g(T) \tag{27}$$

where $\sigma_{q,max,20}$ is the maximum heat rate at 20 $^{\circ}$C. The function $g(T)$ frequently used is an Arrhenius type function,

$$g(T) = \mathrm{e}^{-\frac{E_a}{RT}} \tag{28}$$

where R is the universal gas constant, 8.314 J/mol $\cdot$ K, E_a is the activation energy. Note that in this equation the temperature should be given in K for consistent units. Joining Eq. (27) with Eq. (26), the heat current density released is expressed by,

$$\sigma_q(\alpha, T) = \sigma_{q,max,20} f(\alpha) g(T) \tag{29}$$

Noting out that the heat source rate expressed in Eq. (29) can be also written by taking the derivative of Eq. (25) with respect to time, resulting in

$$\sigma_q = Q_{max} \dot{\alpha} \tag{30}$$

where Q_{max} is the maximum energy density released in J/m^3, i.e. material constant, and the change of reaction degree is represented by,

$$\dot{\alpha} = A(\alpha) g(T). \tag{31}$$

Ulm and Coussy (1995) and Cervera et al. (2002) propose that the function $A(\alpha)$ is obtained by a combination of an affinity model of the chemical reaction and a model of permeability of water through the hydrates, the later explicitly defines the chemical affinity given in h^{-1}as,

$$A(\alpha) = \frac{k}{n_0} \left(\frac{A_0}{k\alpha_\infty} + \alpha \right) (\alpha_\infty - \alpha) \, \mathrm{e}^{-\frac{\bar{n}\alpha}{\alpha_\infty}} \tag{32}$$

where A_0 is the initial affinity, k is an additional parameter, n_0 and $\bar{n}$ are material parameters of the permeability model; and $\alpha_\infty < 1$ is the hydration degree at infinity time.

Using the backward finite difference scheme, Eq. (31) becomes,

$$\frac{\alpha_{n+1} - \alpha_n}{\Delta t} = A(\alpha_{n+1}) g(T_{n+1}), \tag{33}$$

so, we can solve for α_{n+1} using an iterative scheme. We can write Eq. (33) as,

$$\Psi(\alpha_{n+1}) = \alpha_{n+1} - \Delta t A(\alpha_{n+1}) g(T_{n+1}) - \alpha_n = 0. \tag{34}$$

Using the Newton-Raphson method, a general iteration is expressed by,

$$\alpha_{n+1}^{i+1} = \alpha_{n+1}^{i} - \frac{\Psi(\alpha_{n+1}^{i})}{\dfrac{\mathrm{d}\Psi}{\mathrm{d}\alpha_{n+1}}(\alpha_{n+1}^{i})} \tag{35}$$

the derivative of Ψ with respect to α_{n+1}^{i} is given by,

$$\frac{\mathrm{d}\Psi}{\mathrm{d}\alpha_{n+}}(\alpha_{n+1}^{i}) = 1 - \Delta t \; g(T_{n+1}^{i}) \frac{\mathrm{d}f}{\mathrm{d}\alpha_{n+1}}(\alpha_{n+1}^{i}) \tag{36}$$

and the derivative of the function $A(\alpha_{n+1})$, shown in Eq. (32), with respect to α_{n+1} is,

$$\begin{aligned}\frac{\mathrm{d}f}{\mathrm{d}\alpha_{n+1}}(\alpha_{n+1}^{i}) = &-\frac{\bar{n}}{\alpha_\infty}\frac{k}{n_0}\left(\frac{A_0}{k\alpha_\infty} + \alpha_{n+1}^{i}\right)\left(\alpha_\infty - \alpha_{n+1}^{i}\right)\mathrm{e}^{-\frac{\bar{n}\alpha_{n+1}^{i}}{\alpha_\infty}} \\ &- \frac{k}{n_0}\left(\frac{A_0}{k\alpha_\infty} + \alpha_{n+1}^{i}\right)\mathrm{e}^{-\frac{\bar{n}\alpha_{n+1}^{i}}{\alpha_\infty}} + \frac{k}{n_0}\left(\alpha_\infty - \alpha_{n+1}^{i}\right)\mathrm{e}^{-\frac{\bar{n}\alpha_{n+1}^{i}}{\alpha_\infty}}\end{aligned} \tag{37}$$

considering that the temperature will be solved using the Picard scheme, the temperature used in Eq. (33) is the average of $\boldsymbol{T}_{n+1}^{i}$ of the nodes in the element in consideration.

2.4 Picard method

The Picard method, or the fixed point method, is a simple iteration scheme based on fixed points. A point, x is said to be fixed when

$$x = g(x) \tag{38}$$

which means that the function does not change the point value, graphically this means that the function $g(x)$ intersects the function $y = x$. The convergence criteria is $|g'(x)| \leq 1$. Finding the fixed point of $g(x)$ is the same to finding the solution to $f(x) = 0$, where $x = g(x)$ is just an alternative form of the former.

The iterative scheme is formed as,

$$x^{i+1} = g(x^{i}) \tag{39}$$

graphically we can interpret it as: first with an initial guess x^0, we find $g(x^0)$, by tracing a line from this point into the $y = x$ line we find x^1. The next iteration we compute $g(x^1)$ by tracing a line from $y = x$ into the $g(x)$ curve, the process continues until the solution is close enough if it converges. Graphically the process above is represented by a spiral getting closer and closer to the solution.

This method is applied for solution of finite element equations in the literature such as Reddy (2004, p. 440) and Reddy and Gartling (2010, p. 485). In order to solve Eq. (21) as

$$\boldsymbol{\Psi}(\boldsymbol{T}_{n+1}) = 0, \tag{40}$$

where,

$$\boldsymbol{\Psi}(\boldsymbol{T}_{n+1}) = \hat{\boldsymbol{K}}\boldsymbol{T}_{n+1} - \hat{\boldsymbol{F}}(\boldsymbol{T}_{n+1}). \tag{41}$$

we use the following iterative scheme,

$$\boldsymbol{T}_{n+1}^{i+1} = \left[\hat{\boldsymbol{K}}\right]^{-1} \hat{\boldsymbol{F}}(\boldsymbol{T}_{n+1}^{i}) \tag{42}$$

here, i is the iteration index. The initial guess is taken as $\boldsymbol{T}_{n+1}^{0} = \boldsymbol{T}_n$, which is the converged solution from the previous time step, n. The iteration stops when the convergence criteria is satisfied,

$$\frac{||\boldsymbol{T}_{n+1}^{i+1} - \boldsymbol{T}_{n+1}^{i}||}{||\boldsymbol{T}_{n+1}^{i+1}||} < \epsilon, \tag{43}$$

where ϵ is a given tolerance.

3 COMPUTATIONAL ASPECTS

The following algorithm was implemented in Python programming language. The first loop, on line 5, goes over the time steps. Then, on line 9, there is a loop that goes over all elements in order to build element matrices. In each element there is a function, line 10, that computes the reaction degree using a Newton-Raphson scheme. When all element matrices are created and assembled into a global matrix, the linear system generated by the Picard scheme is solved in line 25. If the difference between iterations is small enough, the solution is stored and the next time step starts.

4 VERIFICATION

4.1 Steady state

The verification of the solver for the steady state thermal problem will be done by using the example presented in Nithiarasu et al. (2016, p. 144). In this example, a single four nodes element is loaded with all boundary conditions and with internal heat source. In the bottom side there is an adiabatic condition, $q_h = 0$, on the left side there is a heat current density going out the domain, $q_h = 2\mathrm{W/cm^2}$, on the right side there is a fix temperature assigned, $\bar{T} = 100^{\circ}\mathrm{C}$, and on the top there is a convective boundary condition with the surface condutance coefficient equals to $h = 1.2\mathrm{W/cm^2 \cdot {}^{\circ}C}$ and the air temperature equals to $T_a = 30^{\circ}\mathrm{C}$. The conductivity property of the material is $\lambda = 1.2\mathrm{W/cm \cdot {}^{\circ}C}$ and the internal heat source current density is $\sigma_q = 1.2\mathrm{W/cm^3}$.

The temperature field and the geometry are shown in Fig. 1, the nodal temperature is $T = [85.961, 100., 100., 36.346]$, which is the same solution found by Nithiarasu et al. (2016).

4.2 Transient case

The transient case implementation is verified with a simple problem described in Bofang (2014, p. 183). The problem consists of rectangular domain with dimensions $10x4$ m where the temperature is fixed on both lateral sides at 10 °C. The initial temperature is set to 20 °C, and the diffusivity is equal to $a = 0.10\ \mathrm{m^2/d}$, which was converted to $\mathrm{m^2/s}$. The results are shown in Fig. 2, from which we can observe the diffusion of thermal energy from its initial state at 20 °Cto a more distributed state considering the boundaries fixed temperature.

Algorithm 1 Thermal problem analysis

procedure TRANSIENT SOLVER(t_{int}, dt, T, T_0)
  $T_{np} \leftarrow T_0$ ▷ Initial values
  $\alpha_{np} \leftarrow [0, 0, ..., 0]$ ▷ For all elements
  $N \leftarrow t_{int}/dt$ ▷ Number of steps
  for n in range N **do**
    $t \leftarrow n\Delta t$
    $T_{ip} \leftarrow T_{np}$ ▷ Initialize iteration for the temperature
    while $error \leq 10^{-8}$ **do**
      for e in elements **do** ▷ Build element matrices
        procedure REACTION DEGREE($\alpha_{np}[e], T_{ip}, dt$)
          $\alpha_{ip} \leftarrow \alpha_{np}[e]$
          while $error \leq 10^{-8}$ **do**
            Ψ, $\frac{\mathrm{d}\Psi}{\mathrm{d}\alpha_{n+1}}$ ▷ According to Eq. (34) and (36)
            $\alpha_{iu} \leftarrow \alpha_{ip} - \Psi / \frac{\mathrm{d}\Psi}{\mathrm{d}\alpha_{n+1}}$
            $\alpha_{ip} \leftarrow \alpha_{iu}$
            $error \leftarrow |\alpha_{iu} - \alpha_{ip}|/|\alpha_{iu}|$
          end while
          $\alpha_{nu} \leftarrow \alpha_{iu}$
        end procedure
        $\dot{\alpha} \leftarrow (\alpha_{nu} - \alpha_{np}[e])/dt$ ▷ Eq. (33)
        $\alpha_{np}[e] \leftarrow \alpha_{nu}$ ▷ Save the element reaction degree
        $P_q \leftarrow \int_{V^e} \boldsymbol{N}^T Q_{max} \dot{\alpha} \, \mathrm{d}V$ ▷ Compute load due internal heat
        $\hat{\boldsymbol{K}}, \hat{\boldsymbol{F}}(T_{ip})$ ▷ Build global matrices, Eq. (23)
      end for
      $T_{iu} \leftarrow \hat{\boldsymbol{K}}^{-1} \hat{\boldsymbol{F}}(T_{ip})$ ▷ Eq. (43)
      $T_{ip} \leftarrow T_{iu}$ ▷ Update iteration
      $error \leftarrow ||T_{iu} - T_{ip}||/||T_{iu}||$
    end while
    $T[:, n] \leftarrow T_{iu}$ ▷ Store converged solution for time n
  end for
end procedure

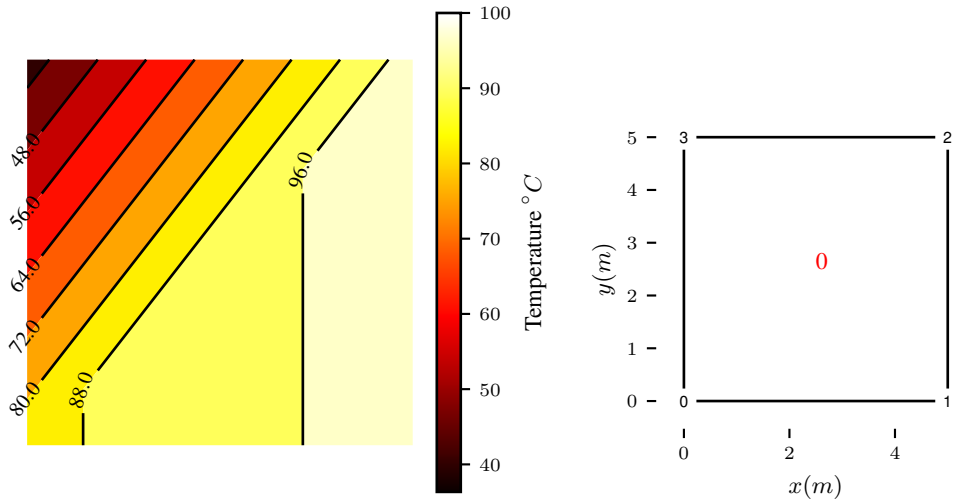

Figure 1: Solution for stationary problem and model domain

4.3 Nonlinear adiabatic

In order to validate the implementation of the heat equation with non linear heat source the numerical result will be compared with experimental data presented in Bentz et al. (1998) and also verified in Cervera et al. (2002). The experiment consists of adiabatic tests of ordinary Portland concrete samples where the temperature were measured at early stages of the curing process. The adiabatic conditions were maintained by a calorimeter which was capable of adjusting the temperature of the sample casing at the same temperature of the surroundings.

The parameters used in the problem are in Table 1. The time increment used was $\Delta t = 168(3600)/50000$s and the sub increment for the reaction degree Newton-Raphson of $\Delta t/10$. The results were compared with experimental results obtained by Bentz et al. (1998). Figure 3 shows the model utilized for the simlation consisting of 4 quad elements. Figure 4 shows the chemical affinity evolution with respect to the reaction degree and the reaction degree evolution through time at the center point. Figure 5 shows the temperature development through time obtained experimentally and via numerical simulation, and on the right, the heat released.

α_∞	k/n_0	$\bar{n}$	A_0/k	E_a/R	Q_{max}	λ	c_p	ρ
	$(10^{-8}\ \mathrm{h}^{-1})$			(K)	$(10^8\ \mathrm{J/m^3})$	$(\mathrm{W/m}\cdot{}^\circ\mathrm{C})$	$(10^6\mathrm{J/kg}\cdot{}^\circ\mathrm{C})$	$(\mathrm{kg/m^3})$
0.66	0.35	6	10^{-5}	5000	2.39	2.6	1	2.33

Table 1: Parameters for simulating adiabatic problem

5 CONCLUSION

The results obtained using the presented model and solution technique agreed with experimental results. The implementation was verified using problems with simple boundary conditions for the stationary and transient case. The internal heat source is modeled as a function of the

reaction degree, which is a new internal variable. The reaction degree is computed considering aspects related to the chemical phenomena such as permeability of water and chemical affinity. The reaction degree depends on the temperature which in turns depends on the reaction degree. Using the Picard scheme, the temperature of the previous step is used to compute the reaction degree of the next step with Newton-Raphson method because the equation is nonlinear with respect to the reaction degree. The two nonlinearities imposed difficulties in convergence of the solution, at the element scale (for the reaction degree) the time iteration was subdivided into smaller ones in order to archive convergence.

REFERENCES

Azenha, Miguel A. D. 2009. *Numerical Simulation of the Structural Behaviour of Concrete since Its Early Ages*. PhD thesis. University of Porto.

Bentz, Dale P., Vincent Waller, and Francois de Larrard. 1998. *Prediction of Adiabatic Temperature Rise in Conventional and High-Performance Concretes Using a 3-D Microstructural Model*. In: *Cement and Concrete Research* 28.

Bofang, Zhu. 2014. *Thermal Stresses and Temperature Control of Mass Concrete*. First edition. OCLC: ocn851417489. Amsterdam ; Boston: Elsevier/BH, Butterworth-Heinemann is an imprint of Elsevier.

Caggiano, A., M. Pepe, E. A. B. Koenders, E. Martinelli, and G. J. Etse. 2012. *Numerical Modeling of Hydration Process and Temperature Evolution in Early Age Concrete*. In: *MECOM 2012: X Argentine Congress on Computational Mechanics, Salta, Argentina, 13-17 November 2012*. Asociación Argentina de Mecánica Computacional.

Cervera, M., R. Faria, J. Oliver, and T. Prato. 2002. *Numerical Modelling of Concrete Curing, Regarding Hydration and Temperature Phenomena*. In: *Computers & structures* 80.18, pp. 1511–1521.

Cervera, Miguel, Javier Oliver, and Tomás Prato. 1999. *Thermo-Chemo-Mechanical Model for Concrete. I: Hydration and Aging*. en. In: *Journal of Engineering Mechanics* 125.9, pp. 1018–1027.

Cohen, E. Richard, Pierre Giacomo, and others. 1987. *Symbols, Units, Nomenclature and Fundamental Constants in Physics*. North-Holland.

De Schutter, G. 2002. *Finite Element Simulation of Thermal Cracking in Massive Hardening Concrete Elements Using Degree of Hydration Based Material Laws*. In: *Computers & Structures* 80.27, pp. 2035–2042.

De Schutter, Geert and Luc Taerwe. 1995. *General Hydration Model for Portland Cement and Blast Furnace Slag Cement*. In: *Cement and Concrete Research* 25.3, pp. 593–604.

Faria, Rui, Miguel Azenha, and Joaquim A. Figueiras. 2006. *Modelling of Concrete at Early Ages: Application to an Externally Restrained Slab*. en. In: *Cement and Concrete Composites* 28.6, pp. 572–585.

Nithiarasu, Perumal, R. W. Lewis, K. N. Seetharamu, and R. W. Lewis. 2016. *Fundamentals of the Finite Element Method for Heat and Mass Transfer*. Second edition. Chichester, West Sussex: Wiley.

Rao, Singiresu S. 2011. *The Finite Element Method in Engineering*. eng. 5. ed. OCLC: 846354670. Amsterdam: Elsevier, Butterworth-Heinemann.

Reddy, J. N. 2004. *An Introduction to Nonlinear Finite Element Analysis*. OCLC: ocm53156584. Oxford ; New York: Oxford University Press.

Reddy, J. N. and David K. Gartling. 2010. *The Finite Element Method in Heat Transfer and Fluid Dynamics*. 3rd ed. CRC Press.

Reinhardt, H.W., J. Blaauwendraad, and J. Jogendijk. 1982. *Temperature Development in Concrete Structures Taking Account of State Dependent Properties*.

Tonti, Enzo. 2013. *The Mathematical Structure of Classical and Relativistic Physics*. Modeling and Simulation in Science, Engineering and Technology. New York, NY: Springer New York.

Ulm, Franz-Josef and Oliver Coussy. 1995. *Modeling of Thermomechanichal Couplings of Concrete at Early Ages*.

Zienkiewicz, O. C. and Robert L. Taylor. 2000. *The Finite Element Method*. 5th ed. Oxford ; Boston: Butterworth-Heinemann.

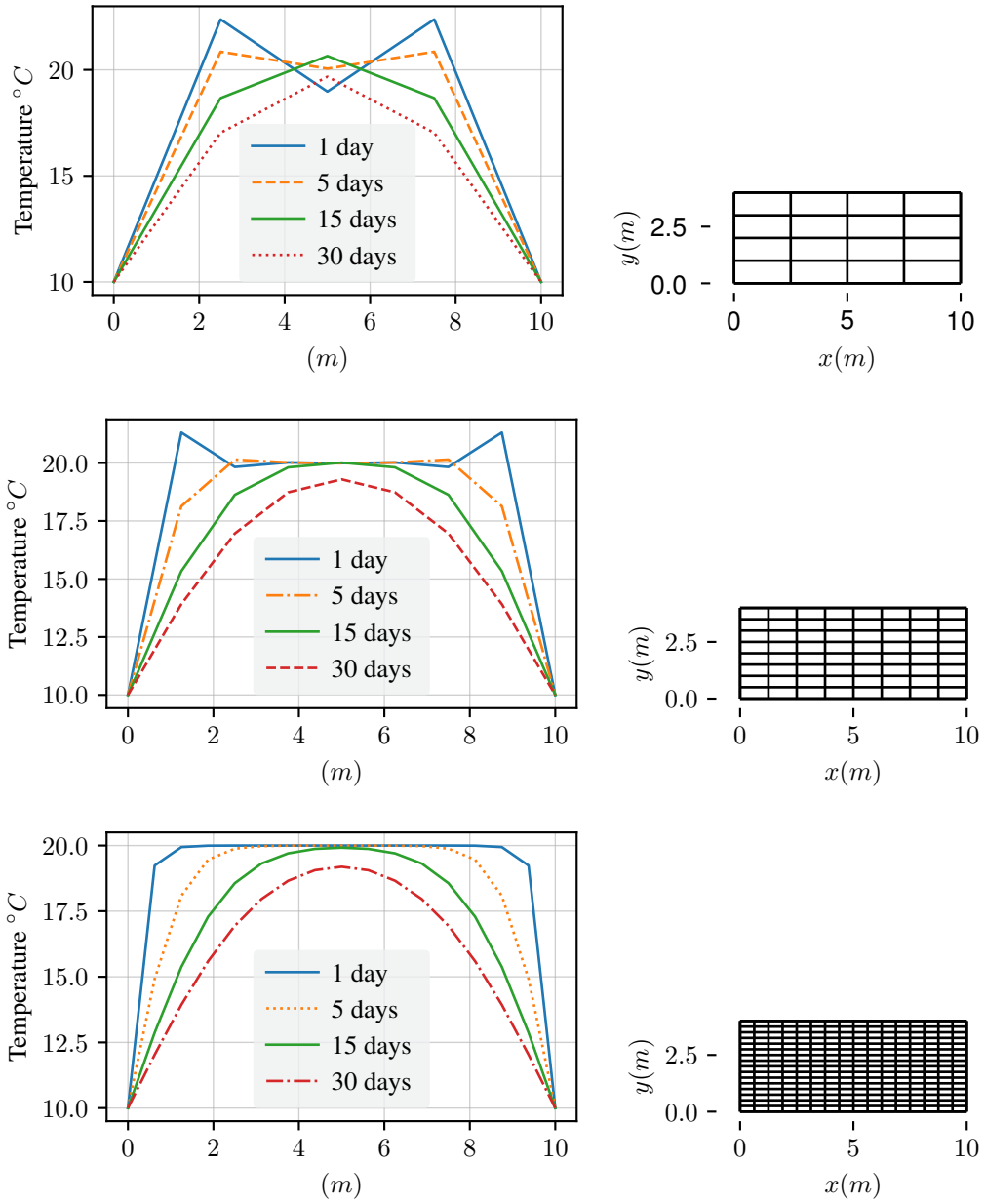

Figure 2: Temperature distribution along the x axis for 16, 64 and 256 elements

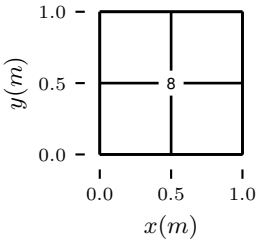

Figure 3: Model utilized for the nonlinear adiabatic case with 4 quad elements and the center node where results were extracted

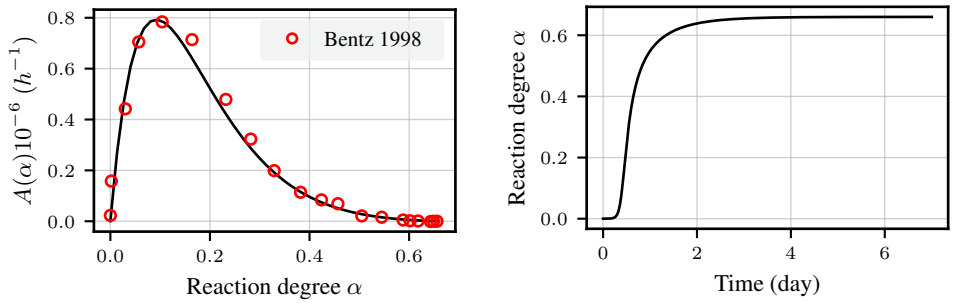

Figure 4: Chemical affinity on the left and the reaction degree on the right. reaction degree considered was the average between elements.

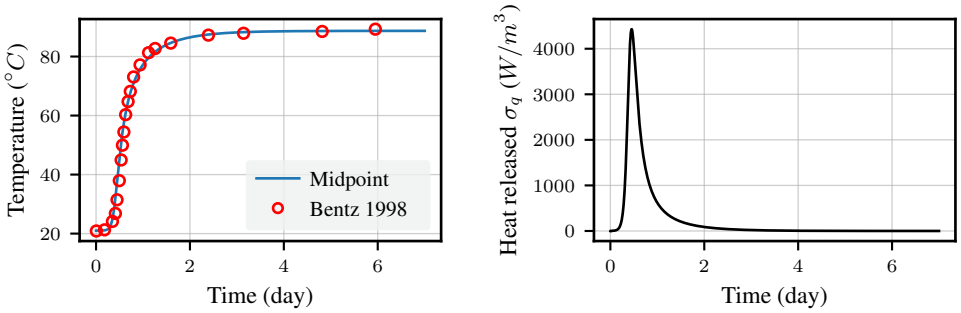

Figure 5: The temperature evolution on mid point compared to experimental results on the left and the heat released averaged between elements.